Analytical and numerical approaches to predict radiated sound power of fluid-loaded cylindrical shells

Yiling Zhang[1,2,*], Weikang Jiang[1], Herwig Peters[2], Nicole Kessissoglou[2]

[1] School of Mechanical Engineering, Shanghai Jiao Tong University, Shanghai, China

[2] School of Mechanical and Manufacturing Engineering, UNSW Australia, Sydney, Australia

ABSTRCT

Prediction of the vibro-acoustic responses of fluid-loaded cylindrical shells is important for underwater vehicles. In this work, a number of analytical and numerical approaches to predict the radiated sound power of a fluid-loaded cylindrical shell are compared. In the first approach, an analytical methodology is used whereby the equations of motion for the cylindrical shell are solved by the method of modal superposition. The shell displacements are represented by a Fourier series and auxiliary functions. The radiation sound power is calculated by integrating the product of the pressure and velocity on the surface of the cylinder. In the second approach, an integrated analytical and numerical approach is implemented whereby the vibrational response of the cylindrical shell is used as an input to a boundary element model. The radiated sound power is subsequently obtained using the boundary element method. In the final approach, a fully-coupled finite element/boundary element model of the fluid-loaded cylinder is developed. Results for the radiated sound power from the various analytical, hybrid analytical/numerical and fully coupled numerical approaches are compared.

Keywords: Radiated sound power, cylindrical shell I-INCE Classification of Subjects Numbers: 21.2.1, 23.1

1. INTRODUCTION

Cylindrical shells are widely used in many applications such as aircraft fuselages, pressure vessels and pipelines. Vibration of cylindrical shells has been extensively investigated by many researchers. Love's thin shell theory was first proposed in 1888 (1). Since then, numerous shell theories have been developed and many are summarised by Leissa (2).

Two common approaches to predict the dynamic responses of cylindrical shells are analytical and numerical methods. The influence of boundary conditions on the dynamic characteristics of cylindrical shells has been analytically investigated by several researchers (3-5). Analytical approaches to predict the sound radiation from cylindrical shells include the modal superposition method (6) and wave propagation method (7). Whilst analytical methods can clearly describe the structural and acoustic responses of cylindrical shells, there are limitations when trying to model shells of complex shapes or shells with irregular internal or external structures.

Using numerical approaches, structures are dispersed into discrete elements. Common numerical approaches include the finite element method (FEM), boundary element method (BEM) and statistical energy analysis. For fluid-structure interaction problems, FEM is generally used to calculate the structural vibration on the fluid-loaded surface and BEM is used to solve the acoustic problem in the exterior acoustic field (8). Numerical FEM/BEM models of fluid-loaded cylindrical shells have been developed to consider excitation by fluctuating forces transmitted to the shell via both structural and fluid paths (9). Recent work using fully coupled FEM/BEM models of a fluid-loaded cylindrical shell has investigated the effects of internal mass distribution and isolation on the radiated sound power (10).

In this work, three approaches to predict the radiated sound power of a fluid-loaded cylindrical shell are compared. In the first approach, an analytical method is used whereby the equations of motion for the cylindrical shell obtained analytically are solved using the method of modal superposition. In the second approach, an integrated analytical and numerical approach is implemented whereby the vibrational response of the cylindrical shell obtained analytically is used as an input to a boundary

[1] drizztzhang@sjtu.edu.cn

element model. The radiated sound power is subsequently obtained numerically using the boundary element method. In the final approach, a fully-coupled finite element/boundary element model of the fluid-loaded cylinder is developed. Results for the radiated sound power from the analytical, hybrid analytical/numerical and fully coupled numerical approaches are compared and discussed.

2. ANALYTICAL APPROACH

Consider a finite cylindrical shell as shown in Figure 1. The radius, thickness and length of the shell are respectively denoted by R, h and L. Four independent springs are placed at each end comprising three linear springs and one rotational spring. Different boundary conditions can be obtained by setting the spring stiffness to different values. For example, a free-free boundary condition can be obtained by setting all the spring stiffness to zero.

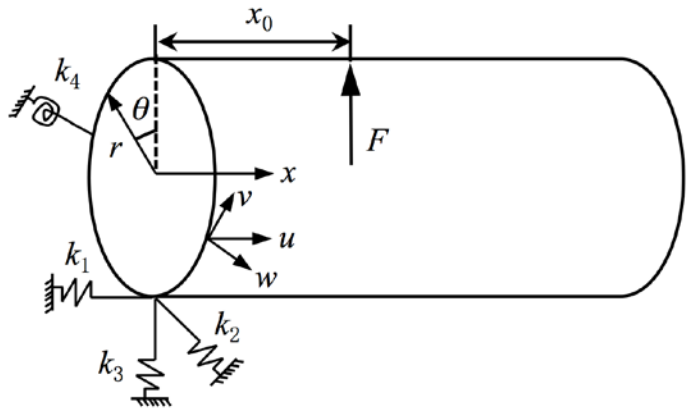

Figure 1 – Schematic diagram of a finite cylindrical shell elastically restrained boundary conditions

2.1 Equations of Motion

The equations of motion for a fluid-loaded cylindrical shell using Donnell-Mushtari thin shell theory are given by (2)

$$\frac{\partial N_x}{\partial x}+\frac{\partial N_{x\theta}}{R\partial\theta}-\rho h\frac{\partial^2 u}{\partial t^2}=0 \tag{1}$$

$$\frac{\partial N_{x\theta}}{\partial x}+\frac{\partial N_{\theta}}{R\partial\theta}-\rho h\frac{\partial^2 v}{\partial t^2}=0 \tag{2}$$

$$\frac{\partial Q_x}{\partial x}+\frac{\partial Q_{\theta}}{R\partial\theta}-\frac{N_{\theta}}{R}-\rho h\frac{\partial^2 w}{\partial t^2}+\frac{1}{K}\left(f_e+p_f\right)=0 \tag{3}$$

where u, v and w denote the shell displacement in the axial, circumferential and radial directions, respectively. ρ is the density of the shell. $K=(Eh)/(1-\mu^2)$ is the in-plane rigidity, where E and μ are respectively the Young's modulus and Poisson's ratio of the shell. p_f is the acoustic pressure of the external fluid acting on the cylindrical shell. Based on the Green's function and the boundary integral equation, the acoustic pressure p_f can be expanded as follows (11)

$$p_f=\frac{\omega^2\rho_0}{\pi}\sum_{n=0}^{\infty}\sum_{m=0}^{\infty}\cos n\theta\int_0^{\infty}\frac{H_n^1(k_rR)}{k_rH_n^{1'}(k_rR)}\frac{S_m(k_x)}{k_m^2-k_x^2}\mathrm{d}k_x \tag{4}$$

ρ_0 is the density of the fluid, H_n is the Hankel function of order n, H_n' is its derivative respect to the argument, k_m is the radial wavenumber, $k_r=\sqrt{k_m^2-k_x^2}$, R is the cylinder radius and

$$S_m(k_x)=\begin{cases}-2k_m\ \sin\left(\dfrac{k_xL}{2}\right)\sin\left[k_x\left(x-\dfrac{L}{2}\right)\right], m \text{ is even}\\ \ 2k_m\cos\left(\dfrac{k_xL}{2}\right)\cos\left[k_x\left(x-\dfrac{L}{2}\right)\right], m \text{ is odd}\end{cases} \tag{5}$$

f_e is an external point force in the transverse direction at a location (x_0,θ_0) which can be expanded as

$$f_e(x,\theta) = \frac{F_e}{\pi L}\sum_{n=0}^{\infty}\sum_{m=0}^{\infty}\cos\lambda_m x_0 \cos\lambda_m x \cos n\theta_0 \cos n\theta \tag{6}$$

where F_e is the magnitude of the exciting force.

2.2 Boundary Conditions

In this study, the shell is considered to be elastically restrained. The boundary conditions for an elastically restrained cylindrical shell are listed in Ref. (12) and are given here for completeness. At $x = 0$ the boundary conditions are

$$k_1 u - N_x = 0, \quad k_2 v - N_{x\theta} = 0, \quad k_3 w - Q_x - \frac{\partial M_{x\theta}}{R\partial\theta} = 0, \quad k_4\frac{\partial w}{\partial x} + M_x = 0 \tag{7}$$

Similarly, at $x = L$ the boundary conditions are

$$k_5 u + N_x = 0, \quad k_6 v + N_{x\theta} = 0, \quad k_7 w + Q_x + \frac{\partial M_{x\theta}}{R\partial\theta} = 0, \quad k_8\frac{\partial w}{\partial x} - M_x = 0 \tag{8}$$

k_1 to k_8 are the spring stiffness as shown in Figure 1. N_x and $N_{x\theta}$ are in-plane forces, Q_x and Q_θ are transverse shear forces, M_x and M_θ are bending moments, and $M_{x\theta}$ is a twisting moment. Definitions for the force and moment expressions in terms of the shell displacements can be found in Refs. (2) and (12).

2.3 General Solutions

Omitting the time harmonic dependency $e^{j\omega t}$, general solutions for the axial, circumferential and radial displacements for a cylindrical shell with elastically restrained boundary conditions can be assumed as (12)

$$u(x,\theta) = \sum_{n=0}^{\infty}\left(\sum_{m=0}^{\infty} A_{mn}\cos\lambda_m x + p_n^u(x)\right)\cos n\theta \tag{9}$$

$$v(x,\theta) = \sum_{n=0}^{\infty}\left(\sum_{m=0}^{\infty} B_{mn}\cos\lambda_m x + p_n^v(x)\right)\sin n\theta \tag{10}$$

$$w(x,\theta) = \sum_{n=0}^{\infty}\left(\sum_{m=0}^{\infty} C_{mn}\cos\lambda_m x + p_n^w(x)\right)\cos n\theta \tag{11}$$

where $\lambda_m = m\pi/L$. As described in Ref. (12), A_{mn}, B_{mn} and C_{mn} are Fourier coefficients of the Fourier series expansions for the shell displacements (12). $p_n^u(x)$, $p_n^v(x)$ and $p_n^w(x)$ are closed form functions used to deal with structural discontinuities and are described in detail in Ref. (13).

The Fourier series expansion coefficients in equations (9) to (11) are determined as follows. The series expansions are truncated to $m = M$ and $n = N$. The total number of unknown Fourier expansion coefficients becomes $3(M+1)(N+1) + 8(N+1)$. The system equations can be assembled by substituting the general solutions given by equations (9) to (11) as well as equations (4) and (6) into the equations of motion given by equations (1) to (3) as well as the boundary conditions given by equations (7) and (8). The final system of equations is a homogenous system of linear equations. Further details on the assembly of the system of equations can be found in Ref. (12).

2.4 Radiated Sound Power

Once the cylindrical shell displacements have been obtained, the radial velocity of the cylindrical shell can be determined from equation (11) as follows

$$\dot{w}(x,\theta) = j\omega\sum_{n=0}^{\infty}\left(\sum_{m=0}^{\infty} C_{mn}\cos\lambda_m x + p_n^w(x)\right)\cos n\theta \tag{12}$$

Using equations (4) and (12), the radiated sound power is obtained by

$$P = \frac{1}{2}\int_0^L\int_0^{2\pi}\mathrm{Re}\left[p_f\dot{w}^*\right]R\mathrm{d}\theta\mathrm{d}x \tag{13}$$

3. NUMERICAL APPROACH

A numerical model using finite elements for the structure and boundary elements to represent the exterior fluid is developed to model the fluid-loaded cylindrical shell with elastically restrained boundary conditions. The coupling conditions at the fluid-structure interface correspond to (i) equilibrium of the acoustic pressure and the normal stress in the structure, and (ii) continuity of the velocities of the fluid particles and the structure in the normal direction on the wetted structural surface. This leads to the following global system of equations (14)

$$\begin{bmatrix} \mathbf{K}-\omega^2\mathbf{M} & -\mathbf{C}_{sf} \\ -i\omega\mathbf{G}\mathbf{C}_{fs} & \mathbf{H} \end{bmatrix} \begin{bmatrix} \mathbf{u} \\ \mathbf{p} \end{bmatrix} = \begin{bmatrix} \mathbf{f}_s \\ \mathbf{p}_i \end{bmatrix} \tag{14}$$

Matrices **K** and **M** are the stiffness and mass matrices of the structure, respectively, and are built using the finite element software package ANSYS. Matrices **H** and **G** are the boundary element method influence matrices obtained through collocation using the BEM software AKUSTA (15). **p** and **u** are vectors with the nodal values for pressure and displacement, respectively. The vectors $\mathbf{f}_s$ and $\mathbf{p}_i$ are the nodal structural forces and the nodal values of the incident pressure field, respectively. $\mathbf{C}_{sf}$ and $\mathbf{C}_{fs}$ are structural-acoustic coupling matrices (14). Once the acoustic pressure on the wetted structural surface and the structural displacement are known, the radiated sound power *P* is obtained by

$$P = \frac{1}{2}\mathrm{Re}\{\mathbf{p}^{\mathrm{T}}\boldsymbol{\Theta}\mathbf{v}_f^*\} \tag{15}$$

where $\mathbf{v}_f$ is the particle velocity and $\boldsymbol{\Theta}$ is the BEM boundary mass matrix (16).

4. RESULTS

The cylindrical shell is 45m long, 6.5m in diameter and has a thickness of 40mm. The shell is made of steel with a density of $\rho = 7800\mathrm{kg/m^3}$, Young's modulus of E=210GPa and Poisson's ratio of $\mu = 0.3$. The shell is submerged in either air or water. Air has a density of $\rho_a = 1.204\mathrm{kg/m^3}$ and speed of sound $c_a = 340\mathrm{m/s}$. Water has a density of $\rho_w = 1000\mathrm{kg/m^3}$ and speed of sound $c_w = 1500\mathrm{m/s}$. Two axial locations along the length of the cylinder for the external transverse point force are considered corresponding to $x_0 = 5\mathrm{m}$ and $x_0 = 22.5\mathrm{m}$. The boundary conditions for the cylindrical shell used in this work are simply supported, corresponding to $k_1 = k_4 = k_5 = k_8 = 0$ and $k_2 = k_3 = k_6 = k_7 = \infty$, where the infinite spring stiffness was achieved using a very large number.

In this study the focus is on the low frequency range up to 50Hz, which corresponds to less than two acoustic waves along the length of the fluid-loaded cylinder. Results for the radiated sound power from the analytical approach, fully coupled numerical model and the hybrid analytical/numerical approach are compared. In the hybrid analytical/numerical method, the radiated sound power is calculated using the analytically obtained structural surface displacement as an input for the BEM software AKUSTA..

The radiated sound power of the cylindrical shell in air and in water for the two different point force excitation locations are presented in Figures 2 to 5. The peaks in the radiated sound power correspond to axial and circumferential modes of the cylindrical shell. When the transverse point force is located halfway along the length of the shell at $x_0 = 22.5\mathrm{m}$, there are less peaks visible. This is due to the fact that for simply supported boundary conditions, midway along the length corresponds to a nodal location for every even integer axial mode number m. As a result, in Figures 3 and 5 there are around half the number of peaks compared to Figures 2 and 4, respectively.

In Figures 2-5, results for the radiated sound power from the three approaches are shown to match reasonably well. The radiated sound power predicted analytically and using the hybrid analytical/numerical approach is in perfect agreement. However, there are some discrepancies with the results obtained numerically using the fully coupled FEM/BEM approach. This discrepancy increases for the shell in water (Figures 4 and 5). Compared with the numerical results, the analytical model does not capture all of the resonant peaks. This error may be attributed to the truncation of the order of the circumferential modes used in the analytical model and will be investigated further. Since the radiated sound power obtained analytically and using the hybrid analytical/numerical approach are in perfect agreement, it is identified that discrepancies in the analytical results are attributed to errors in the prediction of the structural response and not the radiated sound power.

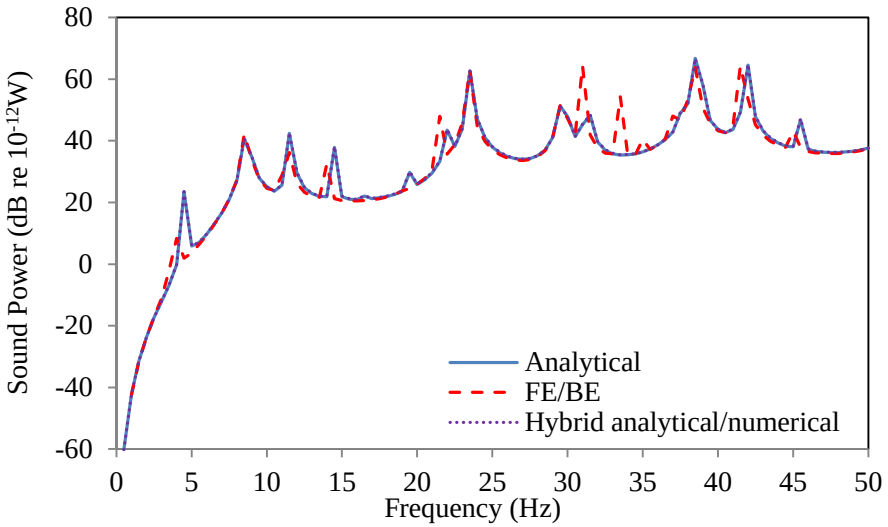

Figure 2 – Sound power from the cylindrical shell in air for a transverse point force at $x_0 = 5\text{m}$

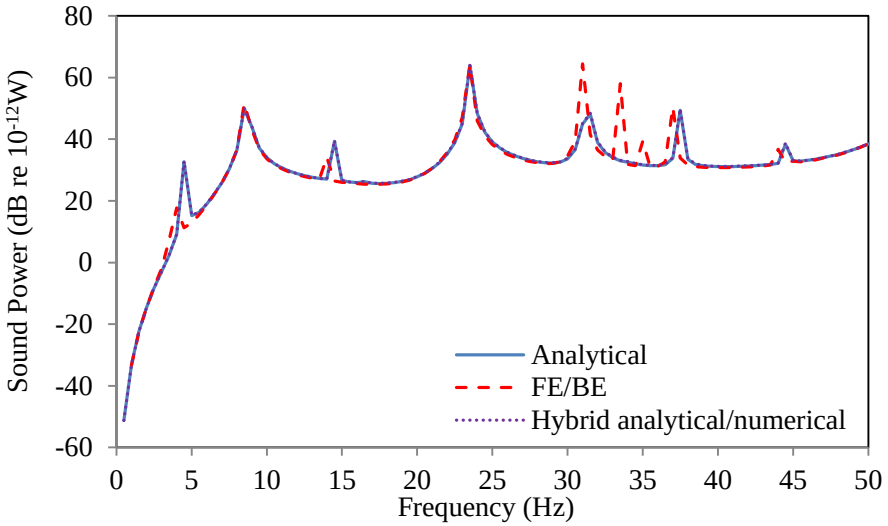

Figure 3 – Sound power from the cylindrical shell in air for a transverse point force at $x_0 = 22.5\text{m}$

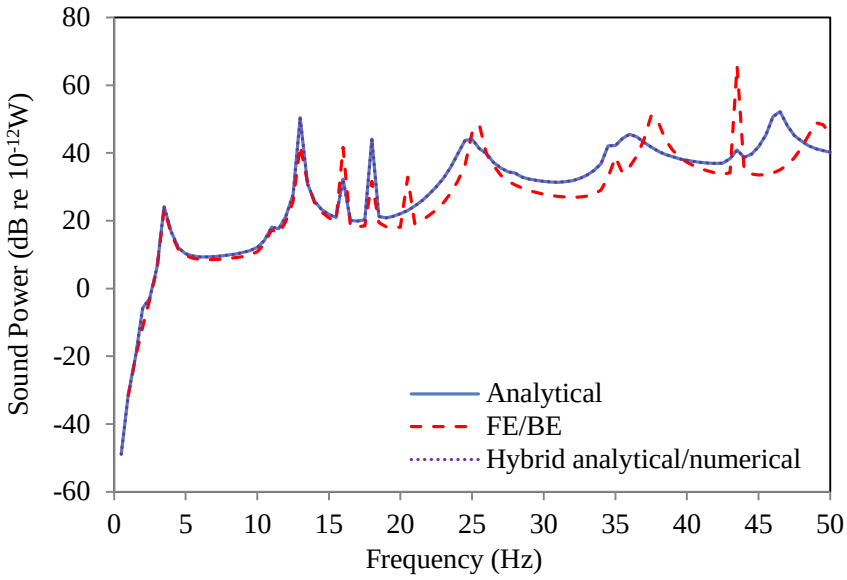

Figure 4 – Sound power from the cylindrical shell in water for a transverse point force at $x_0 = 5\text{m}$

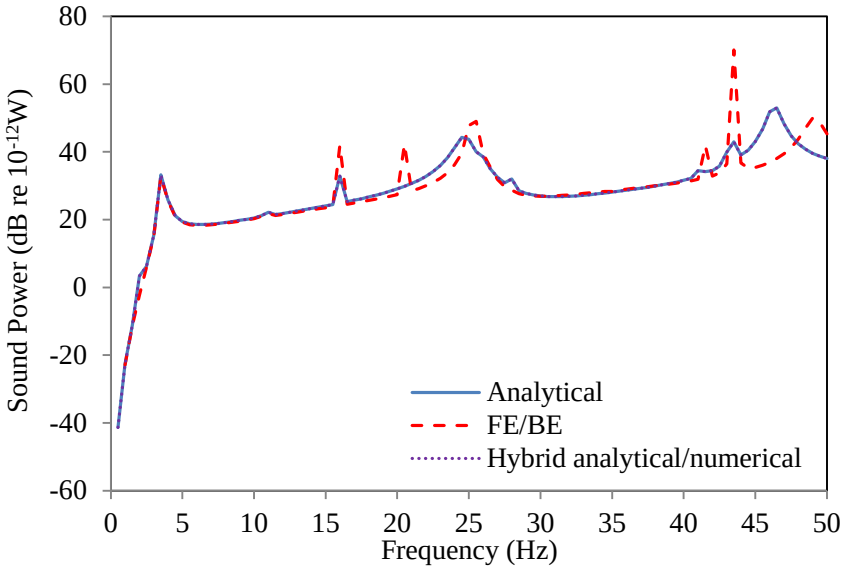

Figure 5 – Sound power from the cylindrical shell in water for a transverse point force at $x_0 = 22.5\text{m}$

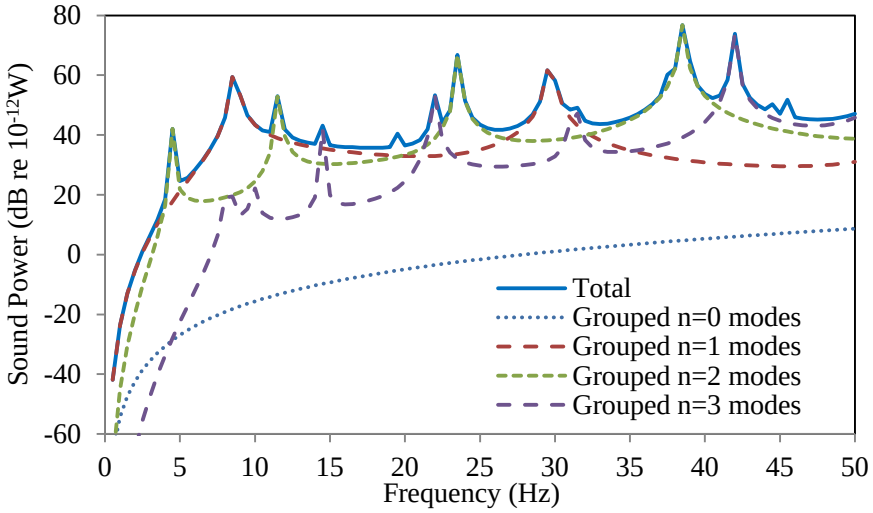

Figure 6 – Sound power and modal contributions from grouped circumferential modes for the cylinder in air

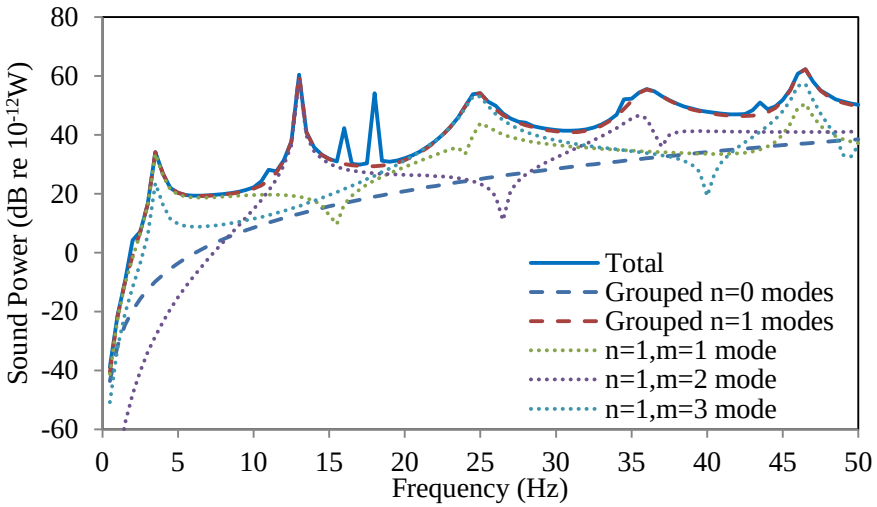

Figure 7 –Sound power and modal contributions from grouped and individual circumferential modes for the cylinder in water

Figures 6 and 7 present the total radiated sound power and modal contributions to the radiated sound power obtained analytically for the cylinder in air and in water, respectively, for a transverse point force located at $x_0 = 5\text{m}$. Unlike using numerical methods, the individual circumferential modes *n* can be easily observed using the analytical approach. For the cylindrical shell in air (Figure 6), the sound power from grouped $n = 0$ modes, grouped $n = 1$ modes, grouped $n = 2$ modes and grouped $n = 3$ modes are also shown. Both Figures 6 and 7 show that for the cylindrical shell under transverse point force excitation, the circumferential $n = 0$ axisymmetric breathing modes are hardly excited. For the frequency range considered, only the $n \leq 3$ modes contribute to the overall sound power. When the cylindrical shell is submerged in water (Figure 7), the effect of the heavy fluid loading has both a mass and damping effect on the structural responses of the cylindrical shell, respectively leading to a decrease of the resonant frequencies and a reduction of the sound power amplitude. Furthermore, the majority of the resonant peaks in Figure 7 correspond to successive circumferential $n = 1$ bending modes of the cylindrical shell. In this figure, the grouped $n = 1$ modes as well as the individual axial modes for the $n = 1$ modes are also presented. The physical insight into the individual modal contributions to the total radiated sound power can allow for more efficient application of noise and vibration control treatments.

5. SUMMARY

The radiated sound power for a fluid-loaded cylindrical shell with simply supported boundary conditions from analytical, hybrid analytical/numerical and fully coupled numerical approaches are presented and compared. The analytical approach was solved by the method of modal superposition using Fourier series with auxiliary functions. The numerical approach consisted of a fully coupled finite element/boundary element model. Comparing results for both techniques with those from a hybrid analytical/numerical approach showed that the radiated sound power calculated using either technique gives the same result. However, the results for the cylinder structural responses obtained analytically and numerically slightly differed. An advantage in using the analytical approach is that the individual contributions from cylindrical shell axial and circumferential modes can be easily observed.

REFERENCES

1. Love AEH. The small free vibrations and deformation of a thin elastic shell. Phil Trans Roy Soc Lon A. 1888;179: 491-546.
2. Leissa, AW. Vibration of Shells. American Institute of Physics. Woodbury, New York, USA; 1993.
3. Laulagnet B, Guyader J. Sound radiation from finite cylindrical coated shells, by means of asymptotic expansion of the three-dimensional equations for coating. J Acoust Soc Am. 1994;96(1):277-286.
4. Burroughs CB. Acoustic radiation from fluid-loaded infinite circular cylinders with doubly periodic ring supports. J Acoust Soc Am. 1984;75(3): 715-722.
5. Forsberg K. Influence of boundary conditions on the modal characteristics of thin cylindrical shells. AIAAJ. 1964;2:2150-2157.
6. Soedel W. A new frequency formula for closed circular cylindrical shells for a large variety of boundary conditions. J Sound Vib. 1980;70:209-217.
7. Zhang XM, Liu GR, Lam KY. Vibration analysis of thin cylindrical shells using wave propagation approach. J Sound Vib. 2001;239:397-403.
8. Mackerle J. Finite- and boundary-element linear and nonlinear analyses of shells and shell-like structures - A bibliography (1999-2001). Fin Elem An Des. 2002;38(8):765-782.
9. Merz S, Kinns R, Kessissoglou NJ. Structural and acoustic responses of a submarine hull due to propeller forces. J Sound Vib. 2009;325:266-286.
10. Peters H, Kinns R, Kessissoglou N. Effects of internal mass distribution and its isolation on the acoustic characteristics of a submerged hull. J Sound Vib. 2014;333:1684-1697.
11. Guanmo X, Dongping L. Analytical solution of radiated sound pressure of ring-stiffened cylindrical shells in fluid medium. Appl Math Mech. 1995;16(12):1143-1148.
12. Dai L, Yang T, Du J, Li WL, Brennan, MJ. An exact series solution for the vibration analysis of cylindrical shells with arbitrary boundary conditions. Appl Acoust. 2013;74(3):440-449.
13. Li WL. Free vibrations of beams with general boundary conditions. J Sound Vib. 2000;237(4):709-725.
14. Peters H, Marburg S, Kessissoglou N. Structural-acoustic coupling on non-conforming meshes with quadratic shape functions. Int J Num Meth Eng. 2012;91:27-38.
15. Marburg S, Nolte B. Computational Acoustics of Noise Propagation in Fluids - Finite and Boundary Element Methods. Springer;2008.
16. Peters H, Kessissoglou N, Marburg S. Modal decomposition of exterior acoustic-structure interaction. J Acoust Soc Am. 2013;133(5):2668-2677.